ORGANOMETALLICS

Article

pubs.acs.org/Organometallics

Synthesis and Characterization of the Double Salts $[Pt(bzq)(CNR)_2][Pt(bzq)(CN)_2]$ with Significant Pt···Pt and π···π Interactions. Mechanistic Insights into the Ligand Exchange Process from Joint Experimental and DFT Study

Juan Forniés,*[,†] Sara Fuertes,[†] Carmen Larraz,[†] Antonio Martín,[†] Violeta Sicilia,*[,‡] and Athanassios C. Tsipis*[,†,§]

[†]Instituto de Síntesis Química y Catálisis Homogénea (ISQCH), Departamento de Química Inorgánica, CSIC−Universidad de Zaragoza, Pedro Cerbuna 12, 50009 Zaragoza, Spain

[‡]Instituto de Síntesis Química y Catálisis Homogénea (ISQCH), Departamento de Química Inorgánica, CSIC−Universidad de Zaragoza, Escuela de Ingeniería y Arquitectura de Zaragoza, Campus Río Ebro, Edificio Torres Quevedo, 50018, Zaragoza, Spain

[§]Laboratory of Inorganic and General Chemistry, Department of Chemistry, University of Ioannina, 451 10 Ioannina,Greece

Supporting Information

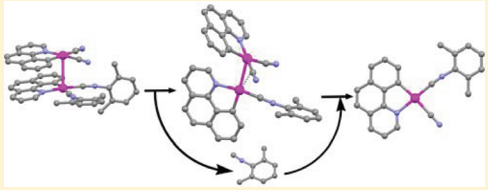

ABSTRACT: Double complex salts (DCSs) of stoichiometry $[Pt(bzq)(CNR)_2][Pt(bzq)(CN)_2]$ (bzq = 7,8-benzoquinolinate; R = *tert*-butyl (**1**), 2,6-dimethylphenyl (**2**), 2-naphtyl (**3**)) have been prepared by a metathesis reaction between $[Pt(bzq)(CNR)_2]ClO_4$ and $[K(H_2O)][Pt(bzq)(CN)_2]$ in a 1:1 molar ratio under controlled temperature conditions (range: −10 to 0 °C). Compounds **1**−**3** have been isolated as air-stable and strongly colored solids [purple (**1**), orange (**2**), red-purple (**3**)]. The X-ray structure of **2** shows that it consists of ionic pairs in which the cationic and anionic square-planar Pt(II) complexes are almost parallel to each other and are connected by Pt−Pt (3.1557(4) Å) and π···π (3.41−3.79 Å) interactions. Energy decomposition analysis calculations on DCSs **1**−**3** showed relatively strong ionic-pair interactions (estimated interaction energies of −99.1, −110.0, and −108.6 kcal/mol), which are dominated by electrostatic interactions with small contributions from dispersion (π···π) and covalent (Pt···Pt) bonding interactions involving the 5d and 6p atomic orbitals of the Pt centers. Compounds **1**−**3** undergo a thermal (165 °C, 24 h) irreversible ligand rearrangement process in the solid state and also in solution at temperatures above 0 °C to give the neutral complexes [Pt(bzq)(CN)(CNR)] as a mixture of two possible isomers (SP-4-2 and SP-4-3). The mechanism of this process has been thoroughly explored by combined NMR and DFT studies. DFT calculations on **1**−**3** show that the existing Pt···Pt interactions block the associative attack of the Pt(II) centers by the coordinated cyanide and/or isocyanide ligands. Moreover, they support a significant transfer of electron density from the anionic to the cationic component (0.20−0.32 |e|), which renders the isocyanide ligand dissociation more feasible than that in the "free-standing" cationic $[Pt(bzq)(CNR)_2]^+$ components as well as the dissociation of the CN^- in *trans* position to the C_{bzq} in the anionic $[Pt(bzq)(CN)_2]^-$ component. Therefore, the first step in the ligand rearrangement pathway is the dissociation of the isocyanide in *trans* position to the C_{bzq}, yielding the $[(RNC)(bzq)(\mu_2\text{-}\eta^1,\eta^1\text{-}CN)Pt\cdots Pt(bzq)(CN)]$ intermediates. The rate-limiting step corresponds to the transformation of these intermediates to the neutral [Pt(bzq)(CN)(CNR)] complexes following a synchronous mechanism involving rupture of the Pt−Pt and formation of the Pt−CN bonds through transition states formulated as $[(RNC)(bzq)Pt(\mu_2\text{-}\eta^1,\eta^1\text{-}CN)Pt(bzq)(CN)]$.

■ INTRODUCTION

Metallophilic interactions between metals with d^8, d^{10}, or s^2 electron configurations in extended linear chains have, for many years, attracted considerable attention.[1−10] Contacts between metals in one-dimensional compounds allow them to behave as efficient conductors with potential application in the field of molecular electronics.[9,11] In addition, intermetallic interactions are the cause of the intense colors exhibited by this type of solid as well as other fascinating features in the optical field.[12−16]

Some of these linear compounds are double complex salts (DCSs) formed by cationic and anionic complexes stacked in an alternate way with metallophilic interactions between metal atoms forming single-atom wide wires.[17−26] The first DCS prepared and characterized was the Magnus salt $[Pt(NH_3)_4][PtCl_4]$, which exists in two forms that can be distinguished by their color.[18] In the green form the platinum atoms show a linear array with Pt−Pt distances of ca. 3.23(2) Å. However, in the Magnus pink salt, as deduced by powder diffraction, the Pt−Pt distance is larger than 5 Å. Compounds $[Pd(NH_3)_4][PdCl_4]$, $[Pt(NH_3)_4][PdCl_4]$, and $[Pd(NH_3)_4][PtCl_4]$,[19−21]

Special Issue: F. Gordon A. Stone Commemorative Issue

Received: October 25, 2011
Published: January 18, 2012

isostructural with the Magnus green salt but exhibiting pink color, and DCSs of the type $[M(NH_2R)_4][MCl_4]$ (M = Pd, Pt) have been also reported.[21,22] The green color seems to be restricted to compounds with the shorter Pt−Pt distances (3.25 Å, R = Me),[20,21] while the pink color might be associated with reduced intermetallic interactions and longer distances (3.62 Å, R = Et).[22,23] In Pt(II) chemistry close attention has been paid to DCSs because of their increasing use in materials science. A large number of heterometallic (Pt−M) DCSs have been synthesized and have sometimes been used as precursors of bi- and polymetallic powders produced by thermal decomposition of these salts, attempting to prepare highly effective heterogeneous catalysts.[27−30] However, the really well-known DCSs are those containing $[Pt(CN)_4]^{2-}$. Compounds such as $[Pt(phen)(CN\text{-}Cyclohexyl)_2][Pt(CN)_4]$[16] and $[Pt(CNR)_4][M(CN)_4]$ (M = Pt, Pd; R = alkyl, aryl)[24−26] have been shown to be vapoluminescent and capable of being incorporated into electronic devices for water vapor and/or volatile organic compound (VOC) sensing applications. Thermal rearrangement of the DCS $[Pt(p\text{-}CN\text{-}C_6H_4\text{-}C_2H_5)_4][Pt(CN)_4]$ in refluxing chloroform or by heating in the absence of solvent gives the neutral complexes *trans*-$[Pt(p\text{-}CN\text{-}C_6H_4\text{-}C_2H_5)_2(CN)_2]$[31] and *cis*-$[Pt(p\text{-}CN\text{-}C_6H_4\text{-}C_2H_5)_2(CN)_2]$,[13] with the *cis* isomer exhibiting vapoluminescent behavior. More recently Drew and co-workers[32] synthesized the neutral $[Pt^{II}(CN\text{-}i\text{-}C_3H_7)_2(CN)_2]$ complex by heating the DCS $[Pt(CN\text{-}i\text{-}C_3H_7)_4][Pt(CN)_4]$ at 190 °C under N_2, and its solid-state characteristics have been investigated to determine the viability of the extended linear chain as a useful benzene sensor.

Ligand exchange processes form part of the most fundamental types of chemical reactions.[33] They have been widely observed in square-planar transition-metal complexes, where they find extensive synthetic applications, and the mechanisms by which they take place have been studied in a few cases.[34−37] Such processes have also been observed in double complex salts, which however have some preparative drawbacks such as limited stability. In spite of this, as far as we know, the mechanism of the ligand rearrangement reactions that DCSs frequently undergo have not been investigated to date.

In our previous work on cyclometalated Pt(II) compounds we prepared luminescent anionic complexes $[Pt(bzq)(CN)_2]^-$ (C^N = bzq, ppy), which could be isolated in two forms: the yellow $[K][Pt(C^N)(CN)_2]$ and the red (bzq) or purple (ppy) $[K(H_2O)][Pt(C^N)(CN)_2]$, which reversibly transform into each other.[38] In addition, compound $[K(H_2O)][Pt(bzq)(CN)_2]$ exhibits vapochromism when it is exposed to VOCs. We have also reported the luminescent cationic complexes $[Pt(bzq)(CNR)_2]ClO_4$ (R = ^{t}Bu, Xyl, 2-Np).[39] Following on with our interest in luminescent cyclometalated Pt(II) compounds we have used the aforementioned complexes to prepare the DCS $[Pt(bzq)(CNR)_2][Pt(bzq)(CN)_2]$ [bzq = 7,8-benzoquinolinate; R = *tert*-butyl (^{t}Bu, **1**), 2,6-dimethylphenyl (Xyl, **2**), 2-naphtyl (2-Np, **3**)], consisting of ionic pairs stabilized by Pt···Pt and $\pi\cdots\pi$ stacking interactions in the solid state. These new DCSs have been found to be metastable species both in solution and in the solid state, eventually evolving to the corresponding neutral species $[Pt(bzq)(CN)(CNR)]$. The transmetalation process by which such a rearrangement takes place has been thoroughly studied by a combined experimental (NMR) and computational (DFT) approach, whereby the rate-limiting step has been assigned and identified.

RESULTS AND DISCUSSION

Synthesis and Characterization of the DCS $[Pt(bzq)(CNR)_2][Pt(bzq)(CN)_2]$. The double complex salts $[Pt(bzq)(CNR)_2][Pt(bzq)(CN)_2]$ [bzq = 7,8-benzoquinolinate; R = *tert*-butyl (^{t}Bu, **1**), 2,6-dimethylphenyl (Xyl, **2**), 2-naphtyl (2-Np, **3**)] were prepared by reaction of $[K(H_2O)][Pt(bzq)(CN)_2]$[38] with an equimolar amount of the corresponding isonitrile complex, $[Pt(bzq)(CNR)_2]ClO_4$,[39] under controlled temperature conditions (see Scheme 1 and Experimental Section) and isolated from the reaction mixtures as air-stable and intensely colored solids [purple (**1**), orange (**2**), red-purple (**3**)]. Other DCSs have been also synthesized previously by a metathesis route[17,27,29,40,41]

Scheme 1. Reactions and Numerical Scheme for NMR Purposes of 1−3

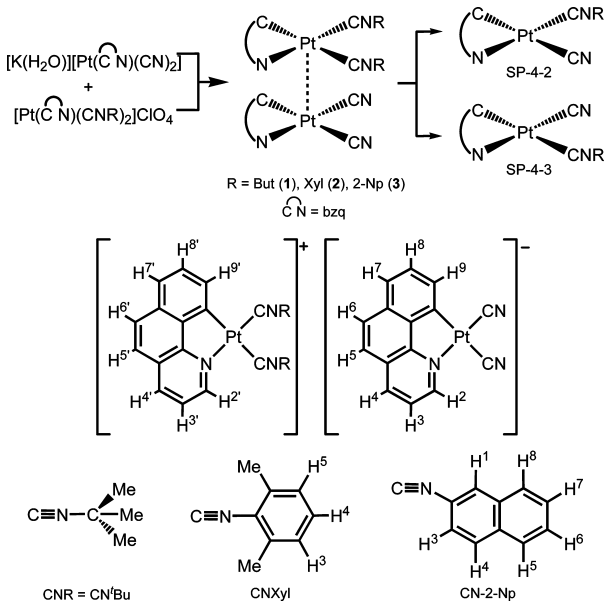

In spite of the similarity of the three compounds, the synthesis conditions are different from each other depending on the nature of the CNR groups, which determines the solubility of the starting complexes, $[Pt(bzq)(CNR)_2]ClO_4$, and that of the DCSs and also the temperature range in which the latter are stable enough to be obtained as pure solids. The DCS $[Pt(bzq)(CNR)_2][Pt(bzq)(^{13}CN)_2]$ [R = ^{t}Bu, **1′**; Xyl, **2′**; 2-Np, **3′**)], containing $^{13}CN^-$, were also prepared by a similar procedure using $(NBu_4)[Pt(bzq)(^{13}CN)_2]$ (**A**) as starting material, with the aim of obtaining a complete characterization of these compounds.

In agreement with the proposed stoichiometry for **1**−**3** their mass spectra show peaks due to the anion $[Pt(bzq)(CN)_2]^-$ and the corresponding cation $[Pt(bzq)(CNR)_2]^+$ operating in a negative and positive mode, respectively (see Experimental Section). Conductivity measurements of freshly prepared methanol solutions (ca. 1×10^{-4} M) of compounds **1**−**3** indicated that they behave as nonelectrolytes [Λ_M (Ω^{-1} cm^2 mol^{-1}): 24, **1**; 20, **2**; 7, **3**].[42] Their IR spectra showed the complete absence of ClO_4^- absorptions[43] and also the ν(C≡N) absorptions corresponding to two terminal cyanide and two

terminal isocyanide ligands, as corresponds to their formula, at frequencies similar to those observed in their starting materials.[38,39] The X-ray study on a single crystal of compound **2** further confirmed the proposed stoichiometry.

As can be seen in Figure 1, compound **2** consists of ionic pairs that are stabilized through electrostatic (Coulombic), covalent Pt···Pt, and dispersive $\pi\cdots\pi$ interactions. The cationic and anionic components of the ionic pairs are square-planar Pt(II) complexes containing the cyclometalated 7,8-benzoquinolinate (bzq) ligand and two xylylisocyanide or two cyanide ligands, respectively, to complete the coordination sphere of the metal atom. Bond angles and distances (Table 1) are in the range of those observed in platinum complexes with C^N-cyclometalated,[44−48] cyanide,[12,13,48−52] and isocyanide[6,13,31,39,53−55] ligands.

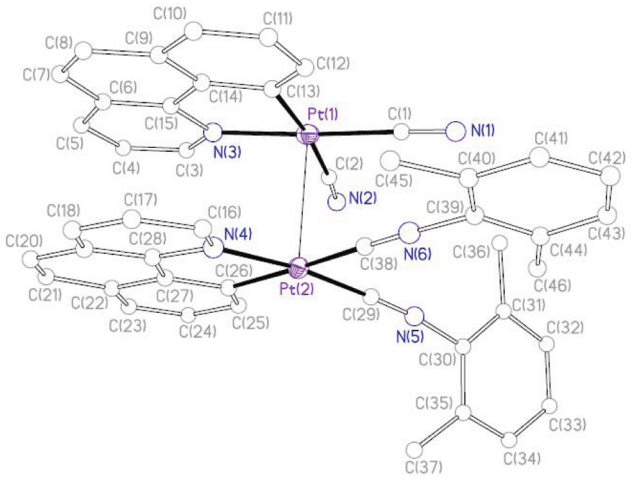

Figure 1. X-ray structure of compound **2**.

Table 1. Structural Data for Compound [Pt(bzq)(CN-Xyl)$_2$][Pt(bzq)(CN)$_2$] (2)

Distances (Å)			
Pt(1)−C(1)	2.0037 (73)	Pt(1)−C(2)	1.9720 (89)
Pt(1)−C(13)	2.0398 (74)	Pt(1)−N(3)	2.0535 (63)
Pt(2)−C(29)	1.9455 (78)	Pt(2)−C(38)	1.9529 (75)
Pt(2)−C(26)	2.0459 (58)	Pt(2)−N(4)	2.0293 (66)
Pt(1)−Pt(2)	3.1557 (4)	C(1)−N(1)	1.1432 (96)
C(2)−N(2)	1.1558 (115)	C(29)−N(5)	1.1756 (102)
C(38)−N(6)	1.1508 (93)	N(5)−C(30)	1.4075 (104)
N(6)−C(39)	1.4051 (81)		
Angles (deg)			
C(1)−Pt(1)−C(2)	92.88 (31)	C(1)−Pt(1)−C(13)	93.28 (28)
N(3)−Pt(1)−C(13)	81.95 (26)	N(3)−Pt(1)−C(2)	91.91 (30)
C(26)−Pt(2)−C(29)	95.24 (27)	C(29)−Pt(2)−C(38)	89.47 (30)
N(4)−Pt(2)−C(26)	82.04 (24)	N(4)−Pt(2)−C(38)	93.16 (28)
Pt(1)−C(1)−N(1)	176.68 (65)	Pt(1)−C(2)−N(2)	175.54 (78)
Pt(2)−C(38)−N(6)	176.45 (65)	Pt(2)−C(29)−N(5)	174.81 (68)
C(29)−N(5)−C(30)	172.50 (77)	C(38)−N(6)−C(39)	170.59 (67)
Pt(2)−Pt(1)−C(1)	85.01 (21)	Pt(2)−Pt(1)−C(2)	94.39 (22)
Pt(2)−Pt(1)−C(13)	84.12 (17)	Pt(2)−Pt(1)−N(3)	95.31 (18)
Pt(1)−Pt(2)−C(26)	84.23 (17)	Pt(1)−Pt(2)−C(29)	87.37 (20)
Pt(1)−Pt(2)−C(38)	97.06 (22)	Pt(1)−Pt(2)−N(4)	98.40 (17)
D−(H)···A	d(D−H)	d(H···A)	d(D···A)	∠(DHA)
O(1)−(H1)···N(2)	0.84 (1)	2.00 (1)	2.777 (10)	153.4 (5)
O(2)−(H2)···O(1)	0.84 (1)	1.96 (1)	2.751 (11)	156.2 (7)

In the ionic pair, the platinum coordination planes are basically parallel to each other (interplanar angle 4.7(2)°) and almost perfectly staggered (torsion angle N(3)−Pt(1)−Pt(2)−C(26): 32.9(3)°; see Figure S1a), presumably minimizing the steric repulsion of the ligands and optimizing the Pt···Pt and $\pi\cdots\pi$ interactions.[56] The Pt(1)−Pt(2) vector is perpendicular to both platinum coordination planes (the angles being 7.7(1)° Pt(1) and 9.0(1)° Pt(2)). The Pt−Pt distance (3.1557(4) Å) is shorter than the accepted limit of 3.5 Å for Pt···Pt interactions[57] and similar to those observed in the crystal structure of other known DCSs such as [Pt(CN)-iso-C_3H_7)$_4$][Pt(CN)$_4$]·16H_2O.[12] The interplanar angle (3.6(1)°) between the bzq fragments and C−C distances as short as 3.41 Å are indicative of significant $\pi\cdots\pi$ interactions[56,58−67] since they are below the upper limit of 3.8 Å for this kind of interaction in aromatic compounds.[57] The cyanide and the isocyanide ligands are almost linearly coordinated to the platinum centers, with bond angles for C and N close to 180°. One of the xylyl groups (C39−C44) is almost coplanar with the Pt(2) coordination plane, the interplanar angle being 6.9(2)°, while the other one (C30−C37) is almost perpendicular (the interplanar angle is 79.9(1)°).

This double salt crystallizes with one and a half molecules of methanol, one of them interacting through H-bonds with one cyanide ligand of the anionic fragment and with the other molecule of methanol in such a way that there are two kinds of hydrogen bonds in the crystal: O−H···N(CN) and O−H···O($OHCH_3$) (see Figure S1b). All distances and angles relating to them are in the range of those observed in other compounds with these kinds of interactions.[12,68]

The ^{1}H NMR spectra of freshly prepared solutions of **1**−**3** show the signals due to the isocyanide ligands in addition to two sets of signals (1:1) corresponding to the bzq ligand in the anionic [Pt(bzq)(CN)$_2$]$^-$ and the cationic [Pt(bzq)(CNR)$_2$]$^+$ fragments (see Scheme 1 and Experimental Section), which could be unambiguously assigned by 2D NMR ^{1}H−^{1}H COSY experiments. The ^{1}H NMR signals of the bzq groups appear significantly upfield shifted with respect to those in their corresponding precursors, suggesting that the noncovalent $\pi\cdots\pi$ interactions are kept in solution. To prove that, the ^{1}H NMR spectra of compound **1** and its precursors (NBu_4)[Pt(bzq)(CN)$_2$][38] and [Pt(bzq)(CN^{t}Bu)$_2$]ClO_4[39] were recorded under the same conditions (solutions 10^{-3} M in CD_2Cl_2, 298 K) and compared (see Figure 2).

As can be seen, the bzq ^{1}H NMR signals in compound **1** appear largely upfield shifted with respect to the corresponding signals in its precursors. This anisotropic shift has been attributed to the $\pi\cdots\pi$ interactions between bzq systems of anions and cations located in close proximity since it cannot be imputed to aromatic solvent-induced shifts (ASIS) nor temperature or concentration.[63,69] The anisotropic shift has sometimes been used as a diagnostic tool in identifying the formation of supramolecular species in solution through $\pi\cdots\pi$ interactions.[70−72] The ^{195}Pt NMR spectra of the more soluble DCSs **1** and **2** were registered, and both show two signals due to the anionic and cationic fragments (see Figure S2 for **1′**) downfield shifted with respect to those in the parent complexes, as can be seen in Table 2. The ^{195}Pt nucleus of the cationic component in **1** is slightly more shielded than that in **2**, as occurs in the starting cationic complexes [Pt(bzq)(CNR)$_2$]PF_6.[39] This feature could be related to the lesser withdrawing

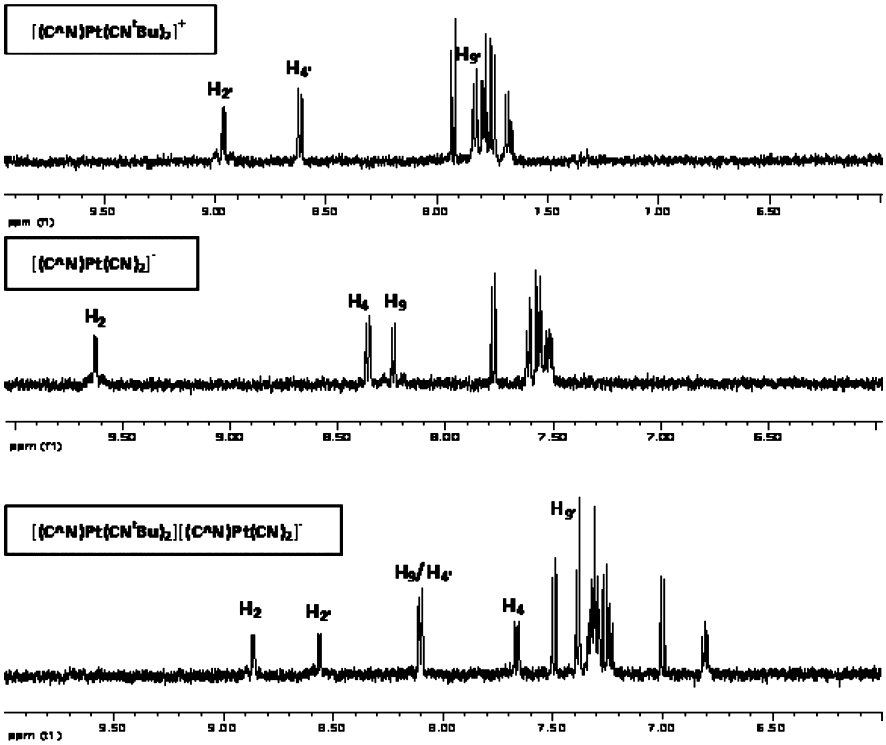

Figure 2. ^{1}H NMR of **1**, $(NBu_4)[Pt(bzq)(CN)_2]$, and $[Pt(bzq)(CN^tBu)_2]ClO_4$ in 10^{-3} M CD_2Cl_2 solution at 298 K, 400 MHz (ppm).

Table 2. ^{195}Pt NMR Data for 1, 2 and Their Starting Complexes[a]

compound	anion	cation
$NBu_4[Pt(bzq)(CN)_2]$[b]	−4103	
$[Pt(bzq)(CN^tBu)_2]PF_6$[b]		−4246
$[Pt(bzq)(CNXyl)_2]PF_6$[b]		−4168
$[Pt(bzq)(CN^tBu)_2]$ $[Pt(bzq)(CN)_2]$ (**1**)[c]	−4034	−4171
$[Pt(bzq)(CNXyl)_2]$ $[Pt(bzq)(CN)_2]$ (**2**)[d]	−4057	−4078

[a] δ ppm, CD_2Cl_2, 298 K, 86.02 MHz. [b] 298 K. [c] 283 K. [d] 278 K.

character of the CN^tBu in relation to CNXyl, in line with the estimated electrophilicity index ω^+ of 1.08 and 1.56 eV for the CN^tBu and CNXyl, respectively, computed at the B3LYP/6-31+G(d,p) level. The higher electrophilicity index ω^+ = 1.99 eV calculated for CN-2-Np should be reflected by a greater electron-withdrawing character of this ligand compared with CNXyl and CN^tBu.

All the above spectroscopic data support the existence of **1**−**3** as DCSs formed by the anionic $[Pt(bzq)(CN)_2]^-$ and the corresponding cationic $[Pt(bzq)(CNR)_2]^+$ components linked together through Pt···Pt and $\pi\cdots\pi$ interactions.

The ^{13}C NMR spectra of the DCSs $[Pt(bzq)(CNR)_2][Pt(bzq)(^{13}CN)_2]$ [R = ^{t}Bu, **1′**; Xyl, **2′**; 2-Np, **3′**)] were also recorded. The chemical shifts and multiplicity of the ^{13}C NMR signals of **1′** greatly resemble those of the parent cyanide compound $(NBu_4)[Pt(bzq)(^{13}CN)_2]$ (**A**): two doublets ($^2J_{C-C}$ = 4.7 Hz) flanked by ^{195}Pt satellites at 143.8 ppm ($^1J_{Pt-C}$ = 852 Hz) and 115.8 ppm ($^1J_{Pt-C}$ = 1428 Hz), which have been assigned to the cyanide *trans* to C_{bzq} and N_{bzq}, respectively, in agreement with the smaller *trans* influence of N with respect to C.[73] Compounds **2′** and **3′** show similar ^{13}C NMR spectra to that of **1′**, although in these cases no C−C coupling was observed. Therefore, the anion−cation interaction seems not to affect the ^{13}C signals of the cyanide groups.

The double complex salts $[Pt(bzq)(CNR)_2][Pt(bzq)(CN)_2]$ [R = ^{t}Bu, **1**; Xyl, **2**; 2-Np, **3**] are not stable for very long in solution at temperatures above 0 °C because each one transforms into the corresponding neutral complex $[Pt(bzq)(CN)(CNR)]$ (R = ^{t}Bu, Xyl, 2-Np). These neutral complexes $[Pt(bzq)(CN)(CNR)]$ result from a ligand rearrangement process, which is a common feature in DCSs.[14] The rate of this process in solution is lower in methanol (the solvent used in the synthesis of **1**−**3**) than in dichloromethane and decreases in the order **2** > **3** > **1**. ^{1}H NMR experiments in dichloromethane (see Figure S3, for **2**) reveal that at 286 K the signals due to the DCSs have completely disappeared in 30 min, 9 h, or 12 h for **2**, **3**, and **1**, respectively, and in their place, the signals due to a mixture of the SP-4-2 and SP-4-3 isomers (see Scheme 1) of the corresponding neutral complex $[Pt(bzq)(CN)(CNR)]$ are observed, with the SP-4-2 being the principal component and the only one present initially. These two isomers can be distinguished by their H^2, H^4, and H^9 resonances, which are very sensitive to the stereochemistry around Pt, by using 2D NMR ^{1}H−^{1}H COSY experiments, although the rest of signals appear partly overlapped. Unfortunately, all our attempts to obtain pure samples of a single isomer of each neutral complex $[Pt(bzq)(CN)(CNR)]$ were unsuccessful.

In the solid state compounds **1**−**3** also undergo a thermal (165 °C, 24 h) irreversible ligand rearrangement process to give the neutral complexes $[Pt(bzq)(CN)(CNR)]$ (R = ^{t}Bu, Xyl, 2-Np) as a mixture of two isomers (SP-4-2, SP-4-3), as was observed by ^{1}H (and/or ^{13}C) NMR. Analogous behavior to **1**−**3** in solution or when they are heated in the absence of solvent has been observed previously for other DCSs such as $[Pt(NH_2R)_4][PtCl_4]$,[22] $[Pt(CNR)_4][Pt(CN)_4]$,[13,31] or $[Pt(bzq)(CN\text{-}2\text{-}Np)_2][Pt(bzq)Cl_2]$.[74]

Structural, Electronic, and Bonding Properties of the DCSs $[Pt(bzq)(CNR)_2][Pt(bzq)(CN)_2]$ and Their $[Pt(bzq)(CN)_2]^-$ and $[Pt(bzq)(CNR)_2]^+$ (R = ^{t}Bu, Xyl, 2-Np)

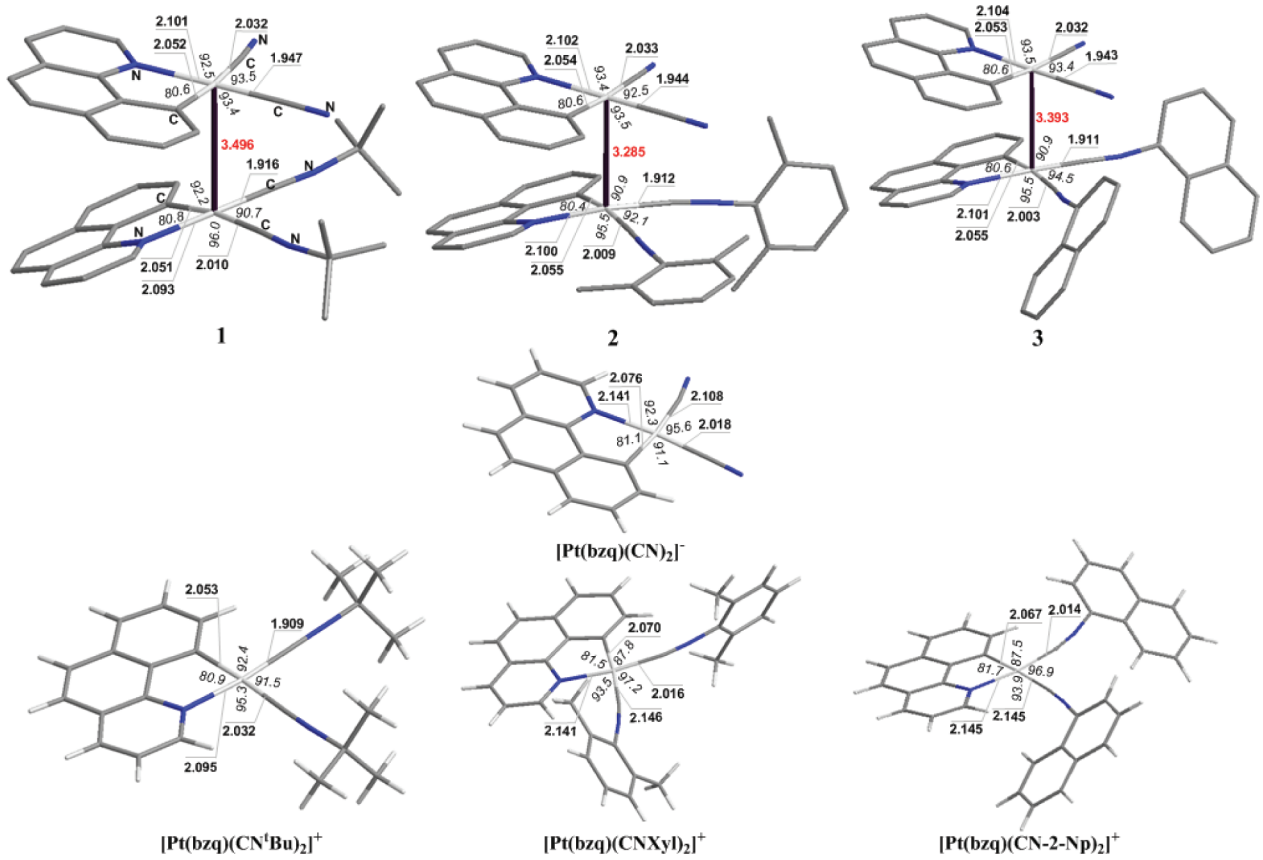

Figure 3. Equilibrium geometries (bond lengths in Å, bond angles in deg) of the DCSs $[Pt(bzq)(CNR)_2][Pt(bzq)(CN)_2]$ (R = ^{t}Bu, **1**; Xyl, **2**; 2-Np, **3**) and their anionic $[Pt(bzq)(CN)_2]^-$ and cationic $[Pt(bzq)(CNR)_2]^+$ components in the gas phase, optimized at the BP86/TZP level of theory.

Components under Vacuum. Prior to the analysis of the mechanism of the ligand redistribution reactions in $[Pt(bzq)(CNR)_2][Pt(bzq)(CN)_2]$ DFT calculations were employed to obtain information about the structures and the electronic and bonding properties of the DCSs $[Pt(bzq)(CNR)_2][Pt(bzq)(CN)_2]$ and their "free-standing" cationic and anionic components. The equilibrium geometries of the DCSs $[Pt(bzq)(CNR)_2][Pt(bzq)(CN)_2]$ and the anionic $[Pt(bzq)(CN)_2]^-$ and cationic $[Pt(bzq)(CNR)_2]^+$ components in the gas phase, optimized at the BP86/TZP level of theory, are shown in Figure 3.

It is noteworthy that the BP86/TZP-optimized bond lengths and bond angles of the DCSs in the gas phase are slightly overestimated with respect to the solid-state X-ray structural data. In particular the estimated Pt−Pt distance was found to be longer by 0.129 Å with respect to the experimental distance of 3.1557(4) Å determined by X-ray crystallography, but in general, the BP86/TZP-optimized structural parameters of **2** are in good agreement with the X-ray structural analysis data: platinum coordination interplanar angle 6.3°; N_{bzq}−Pt−Pt−CNXyl torsion angle 45.4°; angles between the Pt−Pt vector and both platinum coordination planes found to be 7.9° Pt(1) and 9.7° Pt(2). The cyanide and the isocyanide ligands are almost linearly coordinated to the platinum centers, with Pt−C−N bond angles around 175°; one of the xylyl groups is almost coplanar with the Pt coordination plane (interplanar angle was estimated to be 3.1°), while the other one is almost perpendicular, with the interplanar angle found to be 78.2°, in excellent agreement with the X-ray structural data.

The salient structural changes occurring upon formation of the DCSs **1**−**3** from the interaction of the cationic and anionic species are compiled in Table 3. It can be seen that in the ionic pairs both Pt−CN bonds in the anionic $[Pt(bzq)(CN)_2]^-$ component are shortened and the NC−Pt−CN bond angle

Table 3. Structural Changes (bond lengths in Å, bond angles in deg) Accompanying the Formation of the DCSs 1−3 upon Interaction of the Cationic and Anionic Components

structural change	1	2	3
Δ(Pt−CN)[a]	−0.071; −0.076	−0.074; −0.075	−0.075; −0.076
Δ(Pt−N_{bzq})	−0.040	−0.039	−0.037
Δ(Pt−C_{bzq})	−0.024	−0.026	−0.023
Δ(NC−Pt−CN)	−2.1	−3.1	−2.2
Δ(Pt−CNR)[b]	0.007;[c] −0.022[d]	−0.137;[c] −0.104[d]	−0.142;[c] −0.103[d]
Δ(Pt−N_{bzq})		−0.041	−0.044
Δ(Pt−C_{bzq})		−0.015	−0.012
Δ(RNC−Pt−CNR)	−0.08	−5.1	−2.4

[a]With respect to the anionic $[Pt(bzq)(CN)_2]^-$ component. [b]With respect to the cationic $[Pt(bzq)(CNR)_2]^+$ component. [c]The Pt−CNR bond in *trans* position to N_{bzq}. [d]The Pt−CNR bond in *trans* position to C_{bzq}.

becomes smaller with respect to the "free-standing" $[Pt(bzq)(CN)_2]^-$ anion, and the same holds true for the Pt−N_{bzq} and Pt−C_{bzq} bonds. Analogous structural changes occur in the cationic $[Pt(bzq)(CNR)_2]^+$ component of DCSs **2** and **3**. The observed structural changes can be well accounted for the

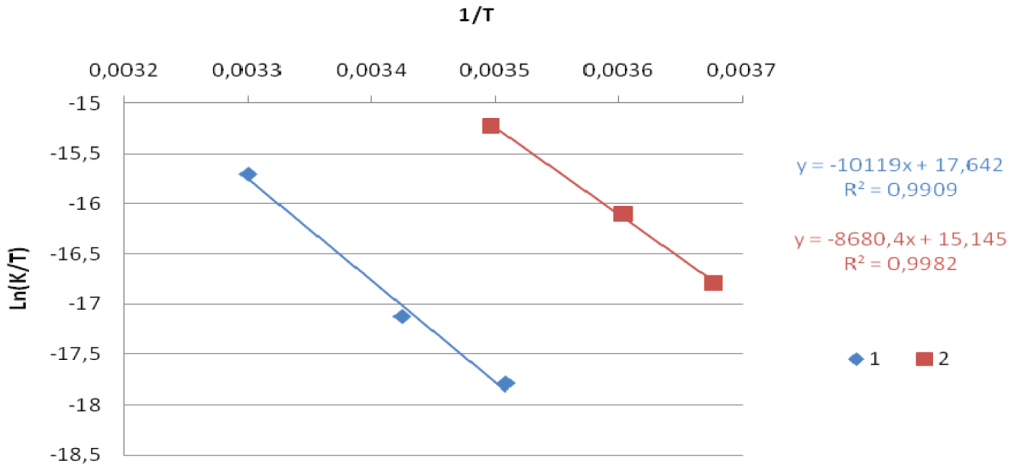

Figure 4. Eyring plots of the rates of the ligand rearrangement process in **1** and **2**.

Pt···Pt interactions existing in **1**−**3**, which support transfer of electron density between the ionic components of the DCSs.

The transfer of electron density from the anionic to cationic component amounted to 0.20, 0.32, and 0.29 |e| for **1**, **2**, and **3**, respectively. The charge transferred is indicative of the contribution of covalent Pt···Pt interactions to the bonding mode following the trend **2** > **3** > **1**. According to the natural bond orbital (NBO) population analysis, the Pt centers of the cationic (anionic) components acquire a positive natural atomic charge of 0.22(0.16), 0.19(0.13), and 0.20(0.15) |e| in **1**, **2**, and **3** DCSs, respectively. Furthermore, the natural electron configuration of the Pt centers of the cationic and anionic components is $5d^{8.73}6s^{0.63}6p^{0.43}$ and $5d^{8.77}6s^{0.66}6p^{0.43}$, respectively, in **1**, $5d^{8.73}6s^{0.61}6p^{0.47}$ and $5d^{8.79}6s^{0.65}6p^{0.44}$, respectively, in **2**, and $5d^{8.72}6s^{0.62}6p^{0.45}$ and $5d^{8.77}6s^{0.65}6p^{0.43}$, respectively, in **3**, illustrating the participation of the 6p atomic orbitals of the Pt centers in the bonding mode as well.

Energy decomposition analysis calculations (EDA), at the SSB-D/TZ2P level, carried out on DCSs **1**−**3** showed relatively strong anion−cation interactions. The interaction energies are estimated to be −99.1, −110.0, and −108.6 kcal/mol for DCSs **1**, **2**, and **3**, respectively. According to EDA, these anion−cation interactions are mainly electrostatic (Coulombic) with small contributions from dispersion forces ($\pi\cdots\pi$-type interactions) and covalent Pt···Pt bonding interactions. The estimated E_{el} component of the interaction energy for **1**−**3** was found to be 72.5, 76.0, and 74.4 kcal/mol, respectively. Accordingly the estimated E_{disp} component of the interaction energy for **1**−**3** was found to be 22.7, 24.2, and 22.4 kcal/mol, respectively, while the E_{cov} component was found to be 3.9, 9.8, and 11.7 kcal/mol, respectively.

Mechanistic Insights into Ligand Exchange Processes in DCSs [Pt(bzq)(CNR)$_2$][Pt(bzq)(CN)$_2$] (R = ^{t}Bu, Xyl, 2-Np) by Combined NMR and DFT Study. Ligand substitution reactions on square-planar Pt(II) complexes usually proceed by an associative mechanism,[75] although clear-cut evidence of a dissociative pathway has been found in ligand exchange or ligand substitution reactions,[34−36] as in complexes of the type *cis*-[PtR$_2$S$_2$] (R = Me, Ph; S = R$_2$S, DMSO),[76] which use the strong labilizing effects of Me and Ph groups to proceed through unsaturated three-coordinated intermediates. However, as far as we know, mechanistic studies of ligand exchange processes in DCSs have been not carried out so far.

As previously mentioned, ^{1}H NMR experiments in dichloromethane revealed that the rate of the ligand exchange process decreases in the order **2** > **3** > **1** and that the DCSs evolved to the corresponding neutral complexes [Pt(bzq)(CN)(CNR)] as a mixture of two isomers, SP-4-2 and SP-4-3, with SP-4-2 being the principal component and the only one present initially.

With the aim of gaining insight into the mechanism of this process and the role of the Pt···Pt and $\pi\cdots\pi$ interactions in the reaction pathway, we studied the ligand rearrangement process undergone by DCSs **1**−**3** by combined experimental and computational calculations. For this purpose ^{1}H NMR spectroscopy was used to follow the processes undergone by compounds **1** and **2** in CD$_2$Cl$_2$ at three different temperatures[77] in the range −1 to +30 °C (see Experimental Section) because the reaction does not work at low temperatures (below −5 °C) and at RT it is very fast, especially for compound **2**. Compound **3** could not be investigated because the resulting neutral complexes precipitate in the NMR tube, which precluded the possibility of obtaining accurate data from the integral values of the NMR signals. The linear Eyring plot, as shown in Figure 4, provides the estimation of the activation parameters ($\Delta H^{\ddagger}$, $\Delta S^{\ddagger}$), which are compiled in Table 4. These studies showed that the rearrangement process on **1** and **2** obeys first-order kinetics (see Figure S4) and that the reaction rate for **1** is lower than for **2** (see rate constants in Table 4).

Table 4. Rate Constants and Activation Parameters for the Ligand Rearrangement Process in 1 and 2

compound	K (s^{-1}) (T)	$\Delta H^{\ddagger}$ (kJ mol^{-1})	$\Delta S^{\ddagger}$ (J K^{-1} mol^{-1})
1	5.3354×10^{-6} (285 K)	84.1 (±8)	−51 (±27)
	1.0624×10^{-5} (292 K)		
	4.5707×10^{-5} (303 K)		
2	1.3885×10^{-5} (272 K)	72.2 (±3)	−72 (±11)
	2.8327×10^{-5} (277 K)		
	7.0134×10^{-5} (286 K)		

Additional experiments proved that (a) DCSs transform into the neutral complexes faster in the presence of free isocyanide (i.e., a 2.26×10^{-3} M solution of DCS **1** in CD$_2$Cl$_2$ at 297 K takes 12 h to transform completely in the neutral complexes and with CN^{t}Bu in 1:1 and 1.2 molar ratio takes 6.5 and 3 h, respectively); (b) at RT complex [Pt(bzq)(CN)$_2$]$^-$ does not react with CNR (R = ^{t}Bu, Xyl; 1:1 or 2:1 molar ratios) to give

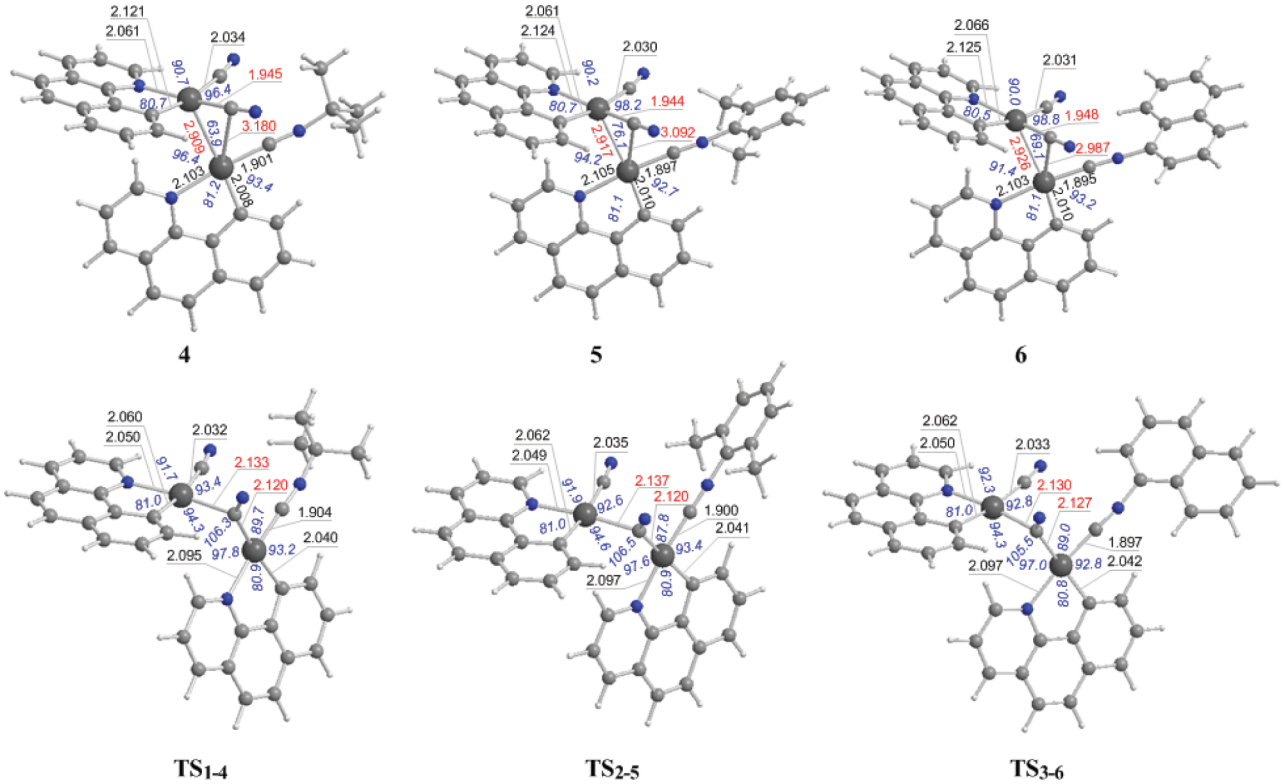

Figure 5. Equilibrium geometries (bond lengths in Å, bond angles in deg) of the DCS intermediates [(RNC)(bzq)(μ_2-η^1,η^1-CN)Pt···Pt(bzq)(CN)] **4**−**6** and the respective transition states in the gas phase optimized at the BP86/TZP level of theory.

the neutral complexes [Pt(bzq)(CN)(CNR)], so the substitution of CN^- by CNR does not take place; and (c) the reactions between $[Pt(bzq)(CNR)_2]^+$ (R = ^{t}Bu, Xyl) and CN^- (1:1 molar ratio) are very quick and mainly render the (SP-4-3)-[Pt(bzq)(CN)(CNR)] isomer with only small traces of the SP-4-2 one. In view of these results it seems plausible to accept that the cation−anion interaction in the DCSs **1** and **2** plays an important role in determining the ligand exchange mechanism.

The strong anion−cation interactions that were described in the previous subsection should block the associative attack of the Pt(II) centers by the coordinated cyanide and/or isocyanide ligands. Moreover, the Pt−Pt interactions are predicted to support a significant transfer of electron density from the anionic to cationic component, which shields the vacant $6p_z$ orbital of the Pt center of the cationic component and hinders nucleophilic attack by the coordinated cyanide ligands of the anionic species. Furthermore, the charge transfer renders the platinum center of the cationic component less electrophilic, and thus the isocyanide ligand dissociation process becomes more feasible. The estimated Pt−CNR energies for the dissociation of the CNR in *trans* position to the C_{bzq} are found to be 107.9, 91.6, and 112.1 kJ/mol for DCSs **1**, **2**, and **3**, respectively. It should be noted that for the "free-standing" cationic $[Pt(bzq)(CN^tBu)_2]^+$, $[Pt(bzq)(CNXyl)_2]^+$, and $[Pt(bzq)(CN\text{-}2\text{-}NP)_2]^+$ components the estimated Pt−CNR bond dissociation energies for the dissociation of the CNR in *trans* position to the C_{bzq} are predicted to be 160.2, 148.1, and 141.8 kJ/mol, respectively. The dissociation of the cyanide ligand in *trans* position to the C_{bzq} in the anionic $[Pt(bzq)(CN)_2]^-$ component is much higher, amounting to 268.6 kJ/mol. Thus, the first step in the ligand rearrangement pathway should correspond to the isocyanide ligand dissociation process yielding the DCS intermediates [(RNC)(bzq)(μ_2-η^1,η^1-CN)Pt···Pt(bzq)(CN)] (R = ^{t}Bu, **4**; Xyl, **5**; 2-Np, **6**).

The optimized equilibrium geometries of the intermediates **4**−**6** with the corresponding transition states, $\mathbf{TS_{1-4}}$, $\mathbf{TS_{2-5}}$, and $\mathbf{TS_{3-6}}$, are shown in Figure 5. In the intermediates **4**−**6** the Pt···Pt interactions are significantly strengthened, as is reflected by the shortening of the Pt−Pt bond lengths by 0.587, 0.368, and 0.467 Å with respect to the Pt−Pt bond lengths of the DCSs **1**−**3**, respectively. Moreover, the C donor atom of the cyanide ligand in *trans* position to N_{bzq} interacts weakly with the platinum atom of the cationic component, forming a weak asymmetric $Pt_1(\mu_2\text{-}CN)Pt_2$ bridge. The C···Pt_2 distances are predicted to be 3.180, 3.092, and 2.987 Å in intermediates **4**, **5**, and **6**, respectively.

The calculated geometric and energetic reaction profiles of the intramolecular ligand rearrangement processes in DCSs **1**−**3** are depicted schematically in Figure 6. As can be seen, the first reaction step involving the dissociation of the isocyanide ligand in *trans* position to the C_{bzq} is endothermic, and the estimated endothermicity was found to be around 92−112 kJ mol^{-1}. The next step of the reaction path involves the migration of the bridging cyanide ligand in intermediates **4**−**6** to the platinum center of the cationic component, affording the SP-4-2 isomers of the neutral [Pt(bzq)(CN)(CNR)] complexes and the neutral three-coordinated [Pt(bzq)(CN)] species with the cyanide ligand in *trans* position to C_{bzq}.

The neutral [Pt(bzq)(CN)] species, being a transient species, easily captures "free" isocyanide ligands to yield the SP-4-2 isomers or rapidly isomerizes to the more stable [Pt(bzq)(CN)] species with the cyanide ligand in *trans* position to N_{bzq}. The geometric and energetic profiles of the isomerization process are depicted schematically in Figure 7.

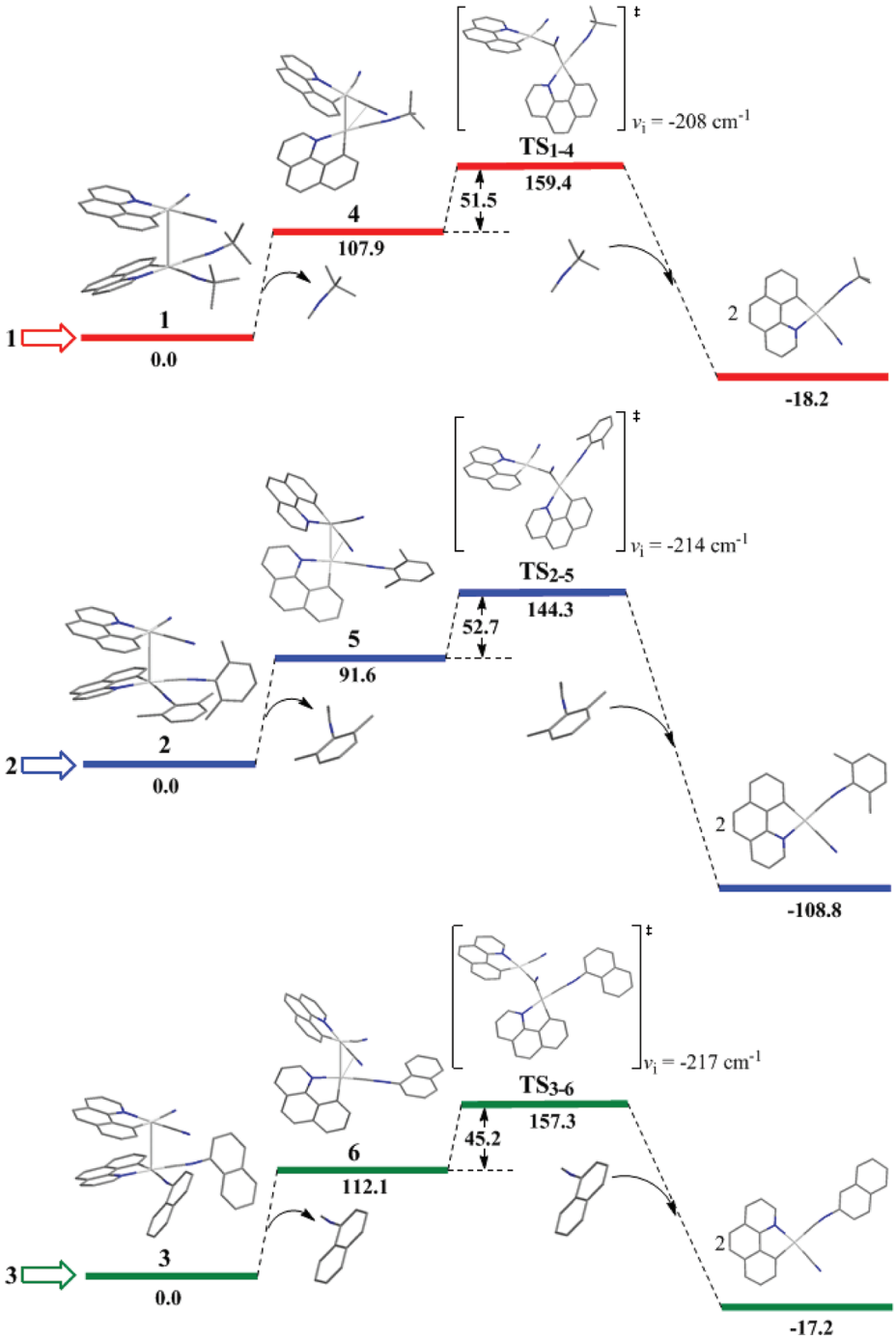

Figure 6. Energetic ($\Delta_R H$, in kJ mol^{-1}) and geometric reaction profiles for the ligand rearrangement processes in DCSs **1**−**3**, computed at the BP86/TZP level of theory.

It can be seen that the isomerization process of the neutral three-coordinated [Pt(bzq)(CN)] species is almost barrierless (activation barrier of 51.5 kJ mol^{-1}) and exothermic by −56.9 kJ mol^{-1}. The more stable three-coordinated isomer easily captures "free" isocyanide ligands to yield the SP-4-3 isomers, thus accounting well for the formation of the mixture of the two isomers detected experimentally.

The rate-limiting step corresponds to the transformation of the intermediates **4**−**6** to the neutral [Pt(bzq)(CN)(CNR)] complexes. The transformation of intermediates **4**, **5**, and **6** proceeds via transition states $\mathbf{TS_{1-4}}$ (ν = 208i cm^{-1}), $\mathbf{TS_{2-5}}$ (ν = 214i cm^{-1}), and $\mathbf{TS_{3-6}}$ (ν = 217i cm^{-1}), surmounting relatively low activation barriers of 159.4, 144.3, and 157.3 kJ mol^{-1}, respectively. In the vibrational modes corresponding to the imaginary frequencies of $\mathbf{TS_{1-4}}$, $\mathbf{TS_{2-5}}$, and $\mathbf{TS_{3-6}}$, the dominant motions involve the movement of the bridging cyanide ligand toward the platinum center of the cationic component. It should be noted that in the transition states the formation of the μ_2-CN bridge enforces the rupture of the Pt−Pt bond. The calculated gas-phase $\Delta S^{\ddagger}$ values for the intramolecular ligand rearrangement processes in DCSs **1**−**3** are predicted to be −153, −208, and −149 J K^{-1} mol^{-1}, respectively, at the BP86/TZP level following the same trend as the experimental values (see Table 4). The negative values of

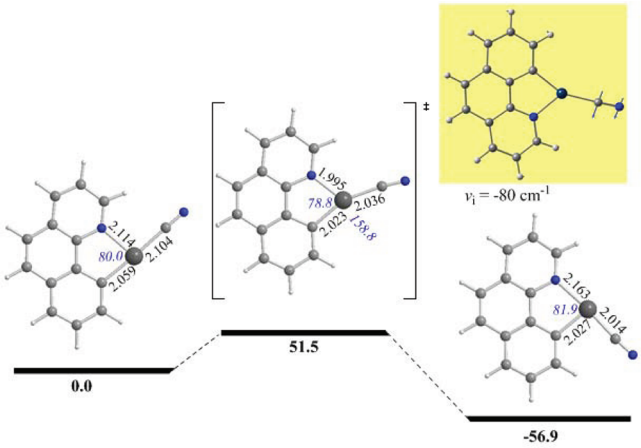

Figure 7. Energetic ($\Delta_R H$, in kJ mol^{-1}) and geometric (bond lengths in Å, bond angles in deg) reaction profiles for the isomerization of the neutral three-coordinated [Pt(bzq)(CN)] species, computed at the BP86/TZP level of theory.

$\Delta S^{\ddagger}$ indicate that the formation of the μ_2-CN bridge precedes the Pt−Pt bond breaking. Overall the transformation process is exothermic; the estimated exothermicities are predicted to be −126.1, −200.4, and −129.3 kJ mol^{-1} for intermediates **4**, **5**, and **6**, respectively (see Figure 7). Furthermore, according to the total energy demand for the formation of the transition states of the DCSs **1**, **2**, and **3** amounting to 159.4, 144.3, and 157.3 kJ mol^{-1}, respectively (Figure 7), the rate of transformation process follows the trend **1** < **3** < **2**, as was experimentally observed. It should be noticed that the relatively large discrepancy between the calculated and experimentally determined "effective" activation enthalpies could be attributed to the fact that gas-phase results, despite the restrictions introduced to the theoretical model, would give a simple relationship to the experimental results obtained in solution. Moreover it is well established that kinetic and thermodynamic results are highly dependent on the functional employed. The proposed mechanism is further supported by the fact that the ligand exchange process is faster in the presence of free isocyanide and the reaction rate increases with the isocyanide concentration.

■ CONCLUSIONS

The double complex salts [Pt(bzq)(CNR)$_2$][Pt(bzq)(CN)$_2$] (bzq = 7,8-benzoquinolinate; R = *tert*-butyl (**1**), 2,6-dimethylphenyl (**2**), 2-naphtyl (**3**)) can be prepared by a metathesis reaction between [Pt(bzq)(CNR)$_2$]ClO$_4$ and [K(H$_2$O)][Pt(bzq)(CN)$_2$] in a 1:1 molar ratio under controlled temperature conditions. The X-ray structure of **2** shows that it consists of ionic pairs stabilized through Pt···Pt and $\pi\cdots\pi$ interactions. Theoretical calculations indicate that, in the DCSs, the bonding mode is dominated by ionic (Coulombic) interactions, but it is also supported by dispersive $\pi\cdots\pi$ and covalent Pt···Pt interactions.

Compounds **1**−**3** are metastable species both in solution and in the solid state, evolving to the corresponding neutral complexes [Pt(bzq)(CN)(CNR)], as a result of a ligand rearrangement process. DFT calculations on **1**−**3** show that the existing Pt···Pt interactions block the associative attack of the Pt(II) centers by the coordinated cyanide and/or isocyanide ligands. They also render the isocyanide ligand dissociation process in DCSs more feasible than for the "free-standing" cationic [Pt(bzq)(CNR)$_2$]$^+$ components and for the dissociation of the CN$^-$ in *trans* position to the C$_{bzq}$ in the anionic [Pt(bzq)(CN)$_2$]− component, so that the first step in the ligand rearrangement pathway is the dissociation of the isocyanide in *trans* position to the C$_{bzq}$, yielding the [(RNC)(bzq)(μ_2-η^1,η^1-CN)Pt···Pt(bzq)(CN)] intermediates. Thus, the rate-limiting step corresponds to the transformation of these intermediates to the neutral [Pt(bzq)(CN)(CNR)] complexes following a synchronous mechanism involving rupture of the Pt−Pt and formation of the Pt−CN bonds through transition states formulated as [(RNC)(bzq)Pt(μ_2-η^1,η^1-CN)Pt(bzq)(CN)]. The total energy demand for the formation of the transition states of the DCSs **1**, **2**, and **3** accounts well for the experimentally observed reaction rate that follows the trend **1** < **3** < **2**.

■ EXPERIMENTAL SECTION

General Procedures and Materials. The starting materials [K(H$_2$O)][Pt(bzq)(CN)$_2$][38] and [Pt(bzq)(CNR)$_2$]ClO$_4$ (R = *tert*-butyl (**1**), 2,6-dimethylphenyl (**2**), 2-naphtyl (**3**))[39] were prepared as described elsewhere. K^{13}CN and KCN were used as purchased from Isotec. Elemental analyses were carried out with a EuroEa elemental analyzer. IR spectra were recorded on a Perkin-Elmer Spectrum 100 FT-IR spectrometer (ATR in the range 250−4000 cm^{-1}). Mass spectral analyses were performed with a Microflex MALDI-TOF Bruker or an Autoflex III MALDI-TOF Bruker instrument.

NMR spectra were recorded on a Varian Unity-300 and Bruker 400 spectrometer using the standard references: SiMe$_4$ for ^{1}H and ^{13}C; Na$_2$PtCl$_6$ in D$_2$O for ^{195}Pt. All of the ^{13}C and ^{195}Pt were proton-decoupled, *J* is given in Hz, and assignments are based on ^{1}H−^{1}H COSY and ^{1}H−^{195}Pt-HMQC experiments.

Synthesis of (NBu$_4$)[Pt(bzq)(^{13}CN)$_2$] (A). (NBu$_4$)[Pt(bzq)(^{13}CN)$_2$] (**A**) was prepared in the same way as (NBu$_4$)[Pt(bzq)(CN)$_2$], but using K^{13}CN. IR (cm^{-1}): ν(C≡N$^-$) 2073s, 2061s. ^{13}C NMR (CD$_2$Cl$_2$, 100.6 MHz, 293 K, δ): 144.2 (d, ^{13}CN$_{trans\text{-}C}$, $^2J_{C-C}$ = 4.7 Hz $^1J_{Pt-C}$ = 832 Hz), 115.8 (d, ^{13}CN$_{trans\text{-}N}$, $^1J_{Pt-C}$ = Hz 1424 Hz).

Synthesis of [Pt(bzq)(CN-^{t}Bu)$_2$][Pt(bzq)(CN)$_2$] (1). To an orange suspension of [Pt(bzq)(CN-^{t}Bu)$_2$](ClO$_4$) (0.200 g, 0.31 mmol) in methanol (25 mL) was added [K(H$_2$O)][Pt(bzq)(CN)$_2$] (0.150 g, 0.31 mmol). The mixture was stirred at 0 °C for 30 min, and then it was allowed to reach room temperature. After 1 h, the orange-red solution was evaporated to dryness and the residue treated with cold CH$_2$Cl$_2$ (10 mL, 0 °C) and filtered through Celite. The resulting solution was evaporated to 2 mL, and diethyl ether (15 mL) was added to it to give pure **1** as a red solid. Yield: 0.22 g, 75%. Anal. Calcd for C$_{38}$H$_{34}$N$_6$Pt$_2$ (964.87): C, 47.30; H, 3.55; N, 8.71. Found: C, 47.26; H, 3.46; N, 8.70. MS(ES+): *m/z* 539 ([Pt(bzq)(CN^{t}Bu)$_2$]$^+$, 100%). MS(ES−): *m/z* 425 ([Pt(bzq)(CN)$_2$]$^-$, 60%). IR (cm^{-1}): ν(C≡NR) 2232s, 2204s, ν(C≡N$^-$) 2122s, 2107s. Λ_M (1.1 × 10^{-4} M, methanol solution): 24 Ω^{-1} cm^2 mol^{-1}. ^{1}H NMR (CD$_2$Cl$_2$, 400.13 MHz, 298 K, δ): 8.8 (dd, ^3J(H2−H3) = 5 Hz, ^4J(H2−H4) = 1 Hz, ^3J(Pt−H2) = 30 Hz, **H2**, bzq), 8.5 (d, ^3J(H2′-H3′) = 5 Hz, ^3J(Pt−H2′) = 35 Hz, **H2′**, bzq), 8.1 (d, ^3J(H9−H8) = 7 Hz, ^3J(Pt−H9) = 44 Hz, **H9**, bzq), 8.0 (d, ^3J(H4′-H3′ = 8 Hz, **H4′**, bzq), 7.6 (dd, ^3J(H4−H3) = 8 Hz, ^4J(H4−H2) = 1 Hz, **H4**, bzq), 7.4 (AB, **H5′**, ^3J(H5′-H6′) = 9 Hz, bzq, ν_A), 7.36−7.2 (m, **H3′**, **H5**, **H6′**, **H7**, **H7′**, **H8**, **H8′**, **H9′**, bzq), 7.0 (AB, **H6**, ^3J(H6−H5) = 9 Hz, bzq, ν_B), 6.8 (dd, ^3J(H3−H4) = 8 Hz, ^3J(H3−H2) = 5 Hz, **H3**, bzq), 1.91 (s, 9H, CH$_3$, CN^t*Bu*), 1.89 (s, 9H, CH$_3$, CN^t*Bu*). ^{195}Pt NMR (CD$_2$Cl$_2$, 86.02 MHz, 283 K, δ): −4034 ([Pt(bzq)(CN)$_2$]$^-$, −4171 ([Pt(bzq)(CN^{t}Bu)$_2$]$^+$). ^{13}C NMR (**1′**, CD$_2$Cl$_2$, 100.6 MHz, 263 K, δ): 143.9 (d, ^{13}CN$_{trans\text{-}C}$, $^2J_{C-C}$ = 5 Hz, $^1J_{Pt-C}$ = 852 Hz), 115.8 (d, ^{13}CN$_{trans\text{-}N}$, $^1J_{Pt-C}$ = 1428 Hz).

Synthesis of [Pt(bzq)(CN-*Xyl*)$_2$][Pt(bzq)(CN)$_2$] (2). To a yellow suspension of [Pt(bzq)(CN-Xyl)$_2$](ClO$_4$) (0.110 g, 0.15 mmol) in methanol (20 mL) was added [K(H$_2$O)][Pt(bzq)(CN)$_2$] (0.072 g, 0.15 mmol) at −10 °C, and the mixture was stirred for 1 h at this temperature to give a bright orange suspension. Then the solvent was evaporated to dryness, and cold H$_2$O (5 mL, 5 °C) added to the

residue to give an orange solid, which was filtered and washed with MeOH (1 mL) and OEt_2 (15 mL), **2**. Yield: 0.11 g, 69%. Anal. Calcd for $C_{46}H_{34}N_6Pt_2$ (1060.96): C, 52.07; H, 3.23; N, 7.92. Found: C, 51.86; H, 3.37; N, 7.94. MS(ES+): m/z 504 ($[Pt(bzq)(CNXyl)_2]^+$, 100%). MS(ES−): m/z 425 ($[Pt(bzq)(CN)_2]^-$, 35%). IR (cm^{-1}): ν(C≡NR) 2205s, 2176s, ν(C≡N$^-$) 2125s, 2114s. Λ_M (1.1×10^{-4} M, methanol solution): 20 Ω^{-1} cm^2 mol^{-1}. ^{1}H NMR (CD_3OD, 400.13 MHz, 298 K, δ): 8.8 (d, ^3J(H2′−H3′) = 5 Hz, **H2′**, bzq), 8.5 (d, ^3J(H2−H3) = 5 Hz, **H2**, bzq), 8.2 (d, ^3J(H4′−H3′) = 8 Hz,, **H4′**, bzq), 8.1 (d, ^3J(H9−H8 = 7 Hz, ^3J(Pt−H9) = 43 Hz, **H9**, bzq), 7.9 (d, ^3J(H4−H3) = 8 Hz, **H4**, bzq), 7.6 (d, ^3J(H9′−H8′ = 7 Hz, ^3J(Pt−H9) = 42 Hz, **H9′**, bzq), 7.5 (AB, **H5′**, ^3J(H5′−H6′) = 9 Hz, bzq, ν_A), 7.5 (AB, **H5**, ^3J(H5−H6) = 9 Hz, bzq, ν_A), 7.44−7.29 (m, **H7**, **H7′**, **H8**, **H8′**, **H3′**), 7.4 (AB, **H6′**, ^3J(H6′−H5′) = 9 Hz, bzq, ν_B), 7.2 (AB, **H6**, ^3J(H6−H5) = 9 Hz, bzq, ν_B), 6.9 (dd, ^3J(H3−H4) = 8 Hz, ^3J(H3−H2) = 5 Hz, **H3**, bzq). ^{195}Pt NMR (CD_2Cl_2, 86.02 MHz, 278 K, δ): −4057 ($[Pt(bzq)(CN)_2]^-$, −4078 ($[Pt(bzq)(CN\text{-}Xyl)_2]^+$). $^{13}C\{^1H\}$ NMR (**2′**,CD_2Cl_2, 100.6 MHz, 253 K, δ): 144.0 (s, $^{13}CN_{trans\text{-}C}$, $^1J_{Pt-C}$ = 845 Hz), 116.1 (s, $^{13}CN_{trans\text{-}N}$, $^1J_{Pt-C}$= 1421 Hz).

Synthesis of [Pt(bzq)(CN-2-Np)$_2$][Pt(bzq)(CN)$_2$] (3). To an orange suspension of $[Pt(bzq)(CN\text{-}2\text{-}Np)_2](ClO_4)$ (0.116 g, 0.15 mmol) in a mixture of $MeCN/H_2O$ (10:10 mL) was added $[K(H_2O)][Pt(bzq)(CN)_2]$ (0.072 g, 0.15 mmol) at −10 °C, and the mixture stirred at −10 °C for 1 h to give a purple suspended solid, which was filtered and washed with H_2O (5 mL), MeOH (5 mL), and OEt_2 (15 mL), **3**. Yield: 0.15 g, 90%. Anal. Calcd for $C_{50}H_{30}N_6Pt_2$ (1104): C, 54.35; H, 2.74; N, 7.61. Found: C, 54.08; H, 2.51; N, 7.63. MS(ES+): m/z 679 ($[Pt(bzq)(CN\text{-}2\text{-}Np)_2]^+$, 100%). MS(ES−): m/z 425 ($[Pt(bzq)(CN)_2]$, 50%). IR (cm^{-1}): ν(C≡NR) 2221s, 2189s, ν(C≡N$^-$) 2119s, 2108s. Λ_M (1×10^{-4} M, methanol solution): 7 Ω^{-1} cm^2 mol^{-1}. ^{1}H NMR (CD_2Cl_2, 400.13 MHz, 298 K, δ): 8.74 (s, **H1**, Np), 8.65 (m, 2H, **H2**, **H2′**, bzq), 8.58 (s, **H3**,Np), 8.20−6.48 (m, 26H, Np/bzq), $^{13}C\{^1H\}$ NMR (**3′**, CD_2Cl_2, 100.6 MHz, 253 K, δ): 143.6 (s, $^{13}CN_{trans\text{-}C}$, $^1J_{Pt-C}$ = 852 Hz), 116.7 (s, $^{13}CN_{trans\text{-}N}$, $^1J_{Pt-C}$ = 1427 Hz).

Kinetic Studies of the Ligand Rearrangement Process in Compounds 1−3. Solutions of compounds $[Pt(bzq)(CNR)_2][Pt(bzq)(CN)_2]$ [R = ^{t}Bu, **1**; Xyl, **2**] in CD_2Cl_2 were prepared at low temperatures and used as samples to follow their conversion into the neutral complexes [Pt(bzq)(CN)(CNR)] by ^{1}H NMR spectroscopy. The spectra were recorded every few minutes at each temperature for both compounds. The rate of reaction was followed in each case by integration of the H^2 signal corresponding to the three identified compounds: $[Pt(bzq)(CNR)_2][Pt(bzq)(CN)_2]$, (SP-4-2)-[Pt(bzq)(CN)(CNR)], and SP-4-3-[Pt(bzq)(CN)(CNR)]. The sum of all three signals was considered as $[DCS]_0$ since the neutral compounds originate from the corresponding DCSs. Plots of $\ln([DCS]_0/([DCS]_t)$ versus time (t) gave a straight line of slope k; plots of $\ln(k/T)$ versus $1/T$ gave slope $\Delta H^{\ddagger}/R$ and intercept $\Delta S^{\ddagger}/R + \ln(k_B/h)$. Errors were determined from error propagation formulas, which were derived from the Eyring equation.[78] The temperature of the NMR probe was calibrated using a methanol temperature standard, and the estimated error in the temperature measurements was 1 K.

Computational Details. The geometries of all stationary points were fully optimized, without symmetry constraints, employing the standard BP86 pure functional as implemented in the ADF 2010.01 program suite.[79] The latter consists of Becke's 1988 functional, which includes the Slater exchange along with corrections involving the gradient of the density[80] combined with a local correlation functional of Perdew that includes gradient corrections.[81] Relativistic effects were treated by applying the zero-order regular approximation (ZORA).[82−86] For optimization of geometries we have used a Slater-type orbitals basis set for all atoms, denoted as TZP, which is a core double-ζ, valence triple-ζ, polarized basis set. This basis set is specially designed for ZORA calculations, primarily to include much steeper core-like functions. Hereafter the method used in DFT calculations is abbreviated as BP86/TZP. All stationary points have been identified as minima (number of imaginary frequencies NImag=0) or transition states (NImag=1). Energy decomposition analysis[87] calculations were performed at the SSB-D/TZ2P level of theory, as implemented in the ADF2010.01 software, while scalar relativistic effects have been considered using ZORA. The SSB-D is a meta-GGA functional that includes dispersion corrections.[88]

X-ray Structure Determination. Suitable crystals for X-ray diffraction studies were obtained by slow diffusion of diethyl ether into a solution of the complexes in methanol. Crystals were mounted at the end of a quartz fiber. The radiation used was graphite-monochromated Mo Kα (λ = 0.71073 Å). X-ray intensity data were collected on an Oxford Diffraction Xcalibur diffractometer. The diffraction frames were integrated and corrected for absorption by using the CrysAlis RED program.[89] The structure was solved by Patterson and Fourier methods and refined by full-matrix least-squares on F^2 with SHELXL-97.[90] All non-hydrogen atoms were assigned anisotropic displacement parameters and refined without positional constraints, except as noted below. All hydrogen atoms were constrained to idealized geometries and assigned isotropic displacement parameters equal to 1.2 times the U_{iso} values of their attached parent atoms (1.5 times for the methyl hydrogen atoms). A well-defined methanol solvent molecule was found in the density maps and refined with occupancy 1. This molecule establishes a H bond with N(2). A second methanol molecule was also found and was refined with a 0.5 partial occupancy. This second methanol established an H bond too, this time with the oxygen atom of the first MeOH molecule, O(1). Full-matrix least-squares refinement of these models against F^2 converged to final residual indices given in Table S4.

■ ASSOCIATED CONTENT

Supporting Information

View of **2**. ^{1}H−^{195}Pt NMR spectrum of compound **1′** in CD_2Cl_2 at 293 K. ^{1}H NMR spectrum showing the transformation of **2** into [Pt(bzq)(CN)(CNXyl)] as a mixture of two isomers at 286 K in CD_2Cl_2. First-order kinetic plots for the ligand redistribution process of **1** in CD_2Cl_2 at 285, 292 and 303 K. First-order kinetic plots for the ligand redistribution process of **2** in CD_2Cl_2 at 272, 277, and 286 K. Cartesian coordinates of all the stationary points (Table S1) and energetic results (Tables S2 and S3). Crystal data and structure refinement for complex **2**·1.5MeOH (Table S4). This material is available free of charge via the Internet at http://pubs.acs.org.

■ AUTHOR INFORMATION

Corresponding Author

*Fax: (+34)976-762189. E-mail: juan.fornies@unizar.es; sicilia@unizar.es; attsipis@uoi.gr.

■ ACKNOWLEDGMENTS

This work was supported by the Spanish MICINN (Projects CTQ2008-06669-C02-01) and the Gobierno de Aragón (Grupo Consolidado: Química Inorgánica y de los Compuestos Organometálicos). A.C.T. thanks the University of Ioannina for the sabbatical leave granted and all his colleagues at the Departamento de Química Inorgánica, Instituto de Ciencia de Materiales de Aragón, Facultad de Ciencias, Universidad de Zaragoza−CSIC, Zaragoza (Spain), for their generous hospitality.

■ DEDICATION

Dedicated to the memory of Prof. F. Gordon A. Stone.

■ REFERENCES

(1) Gliemann, G.; Yersin, H. *Structure and Bonding (Berlin)*; Springer-Verlarg: Berlin, 1985.

(2) Miller, J. S. *Extended Linear Chain Compounds*; Plenum Press: New York, 1982.

(3) Pyykkö, P. *Chem. Rev.* **1997**, *97*, 597.

(4) Mendizábal, F.; Pyykkö, P. *Phys. Chem. Chem. Phys.* **2004**, *6*, 900.
(5) Chen, W.; Liu, F.; Xu, D.; Matsumoto, K.; Kishi, S.; Kato, M. *Inorg. Chem.* **2006**, *45*, 5552.
(6) Sun, Y.; Ye, K.; Zhang, H. X.; Zhang, J.; Zhao, L.; Li, B.; Yang, G.; Yang, B.; Wang, Y.; Lai, S. W.; Che, C. M. *Angew. Chem., Int. Ed.* **2006**, *45*, 5610.
(7) Awaleh, M. O.; Baril-Rolbert, F.; Reber, C.; Badia, A.; Brisse, F. *Inorg. Chem.* **2008**, *47*, 2964.
(8) Zhou, Y.; Chen, W.; Wang, D. *Dalton Trans.* **2008**, 1444.
(9) Mitsumi, M.; Ueda, H.; Furukawa, K.; Ozawa, Y.; Toriumi, K.; Kurmoo, M. *J. Am. Chem. Soc.* **2008**, *130*, 14102 and references therein.
(10) Anderson, B. M.; Hurst, S. K. *Eur. J. Inorg. Chem.* **2009**, 3041.
(11) Cuniberti, G.; Fagas, G.; Richter, K. *Introducing Molecular Electronics*; Springer: New York, 2005.
(12) Buss, C. E.; Anderson, C. E.; Pomije, M. K.; Lutz, C. M.; Britton, D.; Mann, K. R. *J. Am. Chem. Soc.* **1998**, *120*, 7783.
(13) Buss, C. E.; Mann, K. R. *J. Am. Chem. Soc.* **2002**, *124*, 1031−1039.
(14) Daws, C. A.; Exstrom, C. L.; Sowa, J. R. Jr.; Mann, K. R. *Chem. Mater.* **1997**, *9*, 363−368.
(15) Exstrom, C. L.; Pomije, M. K.; Mann, K. R. *Chem. Mater.* **1998**, *10*, 942.
(16) Grate, J. W.; Moore, L. K.; Janzen, D. E.; Veltkamp, D. J.; Kaganove, S.; Drew, S. M.; Mann, K. R. *Chem. Mater.* **2002**, *14*, 1058−1066.
(17) Hayoun, R.; Zhong, D. K.; Rheingold, A. L.; Doerrer, L. H. *Inorg. Chem.* **2006**, *45*, 6120.
(18) Atoji, M.; Richardson, J. W.; Rundle, R. E. *J. Am. Chem. Soc.* **1957**, *79*, 3017.
(19) Rodgers, M. L.; Martin, D. S. *Polyhedron* **1987**, *6*, 225.
(20) Miller, J. R. *Proc. Chem. Soc.* **1960**, 318.
(21) Miller, J. R. *J. Chem. Soc.* **1961**, 4452.
(22) Bremi, J.; Brovelli, D.; Caseri, W.; Hähner, G.; Smith, P.; Tervoort, T. *Chem. Mater.* **1999**, *11*, 977.
(23) Cradwick, M. E.; Hall, D.; Phillips, R. K. *Acta Crystallogr. B* **1971**, *27*, 480.
(24) Drew, S. M.; Janzen, D. e.; Buss, C. E.; MacEwan, D. I.; Dublín, K. M.; Mann, K. R. *J. Am. Chem. Soc.* **2001**, *123*, 8414.
(25) Drew, S. M.; Mann, J. E.; Marquardt, B. J.; Mann, K. R. *Sens. Actuators B* **2004**, *97*, 307.
(26) Drew, S. M.; Janzen, D. E.; Mann, K. R. *Anal. Chem.* **2002**, *74*, 2547.
(27) Shubin, Y. V.; Korenev, S. V. *Zh. Neorg. Khim.* **2002**, *47*, 1812.
(28) Shubin, Y. V.; Korenev, S. V.; Yusenko, K. V.; Korda, T. M.; Venediktov, A. B. *Russ. Chem. Bull. Int. Ed.* **2002**, *51*, 41.
(29) Korenev, S. V.; Makotchenko, E. V.; Plyusnin, P. E.; Baidina, I. A.; Shubin, Y. V. *Russ. Chem. Bull. Int. Ed.* **2006**, *55*, 429.
(30) Zadesenets, A. V.; Filatov, E. Y.; Yusenko, K. V.; Shubin, Y. V.; Korenev, S. V.; Baidina, I. A. *Inorg. Chim. Acta* **2008**, *361*, 199.
(31) Dylla, A. G.; Janzen, D. E.; Pomije, M. K.; Mann, K. R. *Organometallics* **2007**, *26*, 6243.
(32) Drew, S. M.; Smith, L. I.; McGee, K. A.; Mann, K. R. *Chem. Mater.* **2009**, *21*, 3117.
(33) Garrou, P. E. In *Advances in Organometallic Chemistry*; West, F. G. A. S. a. R., Ed.; Academic Press, Inc.: London, U.K., 1984; Vol. 23, pp 95−129.
(34) Wendt, O. F.; Deeth, R. J.; Elding, L. I. *Inorg. Chem.* **2000**, *39*, 5271.
(35) Plutino, M. R.; Scolaro, L. M.; Romeo, R.; Grassi, A. *Inorg. Chem.* **2000**, *39*, 2712.
(36) Romeo, R.; Scolaro, L. M.; Plutino, M. R.; Fabrizi de Biani, F.; Bottari, G.; Romeo, A. *Inorg. Chim. Acta* **2003**, *350*, 143.
(37) Otto, S.; Roodt, A. *J. Organomet. Chem.* **2006**, *691*, 4626.
(38) Forníes, J.; Fuertes, S.; López, J. A.; Martín, A.; Sicilia, V. *Inorg. Chem.* **2008**, *47*, 7166−7176.
(39) Diez, A.; Forníes, J.; Fuertes, S.; Lalinde, E.; Larraz, C.; López, J. A.; Martín, A.; Moreno, M. T.; Sicilia, V. *Organometallics* **2009**, *28*, 1705−1718.
(40) Wu, C.; Chen, H. F.; Wong, K. T.; Thompson, M. E. *J. Am. Chem. Soc.* **2010**, *132*, 3133.
(41) Phillips, V.; Willard, K. J.; Golen, J. A.; Moore, C. J.; Rheingold, A. L.; Doerrer, L. H. *Inorg. Chem.* **2010**, *49*, 9265.
(42) Geary, W. J. *Coord. Chem. Rev.* **1971**, *81*, 7.
(43) Hathaway, B. J.; Underhill, A. E. *J. Chem. Soc.* **1961**, 3091.
(44) Diez, A.; Forniés, J.; García, A.; Lalinde, E.; Moreno, M. T. *Inorg. Chem.* **2005**, *44*, 2443.
(45) Jolliet, P.; Gianini, M.; von Zelewsky, A.; Bernardinelli, G.; Stoeckli-Evans, H. *Inorg. Chem.* **1996**, *35*, 4883.
(46) DePriest, J.; Zheng, G. Y.; Woods, C.; Rillema, D. P.; Mikirova, N. A.; Zandler, M. E. *Inorg. Chim. Acta* **1997**, *264*, 287.
(47) Fernández, S.; Forniés, J.; Gil, B.; Gómez, J.; Lalinde, E. *Dalton Trans.* **2003**, 822.
(48) Forniés, J.; Fuertes, S.; Martín, A.; Sicilia, V.; Gil, B.; Lalinde, E. *Dalton Trans.* **2009**, 2224−2234.
(49) Che, C. M.; He, L.-Y.; Poon, C.-K.; Mak, C. W. *Inorg. Chem.* **1989**, *28*, 3081−3083.
(50) Xia, B.-H.; Che, C. M.; Phillips, D. L.; Leung, K.-H.; Cheung, K. K. *Inorg. Chem.* **2002**, *41*, 3866−3875.
(51) Flay, M.-L.; Vahrenkamp, H. *Eur. J. Inorg. Chem.* **2003**, 1719−1726.
(52) Forniés, J.; Gómez, J.; Lalinde, E.; Moreno, M. T. *Chem.—Eur. J.* **2004**, *10*, 888−898.
(53) Lai, S. W.; Lam, H. W.; Lu, W.; Cheung, K. K.; Che, C. M. *Organometallics* **2002**, *21*, 226.
(54) Vicente, J.; Arcas, A.; Fernández-Hernández, J. M.; Aullón, G.; Bautista, D. *Organometallics* **2007**, *26*, 6155.
(55) Martellaro, P. J.; Hurst, S. K.; Larson, R.; Abbott, E. H.; Peterson, E. S. *Inorg. Chim. Acta* **2005**, *358*, 3377−3383.
(56) Janiak, C. *J. Chem. Soc., Dalton Trans.* **2000**, 3885.
(57) Chen, J. L.; Chang, S. Y.; Chi, Y.; Chen, K.; Cheng, Y. M.; Lin, C. W.; Lee, G. H.; Chou, P. T.; Wu, C. H.; Shih, P. I.; Shu, C. F. *Chem. Asian J.* **2008**, *3*, 2112, and references therein.
(58) Koo, C. K.; Ho, Y. M.; Chow, C. F.; Lam, M. H. W.; Lau, T. C.; Wong, W. Y. *Inorg. Chem.* **2007**, *46*, 3603.
(59) Kui, S. C. F.; Chui, S. S. Y.; Che, C. M.; Zhu, N. *J. Am. Chem. Soc.* **2006**, *128*, 8297.
(60) Ionkin, A. S.; Marshall, W. J.; Wang, Y. *Organometallics* **2005**, *24*, 619.
(61) Poater, A.; Moradell, S.; Pinilla, E.; Poater, J.; Solá, M.; Martínez, M. A.; Llobet, A. *Dalton Trans.* **2006**, 1188.
(62) Ding, J.; Pan, D.; Tung, C. H.; Wu, L. Z. *Inorg. Chem.* **2008**, *47*, 5099.
(63) Lu, W.; Chan, M. C. W.; Zhu, N.; Che, C. M.; Li, C.; Hui, Z. *J. Am. Chem. Soc.* **2004**, *126*, 7639.
(64) Lu, W.; Chan, M. C. W.; Cheung, K. K.; Che, C. M. *Organometallics* **2001**, *20*, 2477.
(65) Steed, J. W.; Atwood, J. L. *Supramolecular Chemistry*; Wiley-Interscience: Chichester, 2000.
(66) Oh, M.; Carpenter, G. B.; Sweigart, D. A. *Organometallics* **2003**, *22*, 1437.
(67) Roesky, H. W.; Andruh, M. *Coord. Chem. Rev.* **2003**, *236*, 91.
(68) Vitoria, P.; Beitia, J. I.; Gutierrez-Zorrilla, J. M.; Saiz, E. R.; Luque, A.; Insausti, M.; Blanco, J. J. *Inorg. Chem.* **2002**, *41*, 4396.
(69) Mitra, A.; Seaton, P. J.; Assarpour, R. A.; Williamson, T. *Tetrahedron* **1998**, *54*, 15489.
(70) Hunter, C. A.; Meah, M. N.; Sanders, J. K. M. *J. Am. Chem. Soc.* **1990**, *112*, 5773.
(71) Yamauchi, Y.; Yoshizawa, M.; Fujita, M. *J. Am. Chem. Soc.* **2008**, *130*, 5832.
(72) Yam, V. W. W.; Chan, K. H. Y.; Wong, K. M. C.; Chu, B. W. K. *Angew. Chem., Int. Ed.* **2006**, *45*, 6169.
(73) Casas, J. M.; Forníes, J.; Fuertes, S.; Martín, A.; Sicilia, V. *Organometallics* **2007**, *26*, 1674.
(74) Diez, A.; Forníes, J.; Larraz, C.; Lalinde, E.; López, J. A.; Martín, A.; Moreno, M. T.; Sicilia, V. *Inorg. Chem.* **2010**, *49*, 3239.

(75) Schmülling, M.; Grove, D. M.; van Koten, G.; van Eldik, R.; Veldman, N.; Spek, A. L. *Organometallics* **1996**, *15*, 1384, and references therein.
(76) Romeo, R. *Comments Inorg. Chem.* **1990**, *11*, 21.
(77) Yang, F. Z.; Wang, Y. H.; Chang, M. C.; Yu, K. H.; Huang, S. L.; Liu, Y. H.; Wang, Y.; Liu, S. T.; Chen, J. T. *Inorg. Chem.* **2009**, *48*, 7639,and references therein.
(78) Morse, P. M.; Spencer, M. D.; Wilson, S. R.; Girolami, G. S. *Organometallics* **1994**, *13*, 1646.
(79) *ADF2010.01* SCM Theoretical Chemistry; Vrije Universiteit: Amsterdam, The Netherlands, 2010.
(80) Becke, A. D. *Phys. Rev. A* **1988**, *38*, 3098.
(81) Perdew, J. P. *Phys. Rev. B* **1986**, *33*, 8822.
(82) van Lenthe, E.; Ehlers, A. E.; Baerends, E. J. *J. Chem. Phys.* **1999**, *110*, 8943.
(83) van Lenthe, E.; Baerends, E. J.; Snijders, J. G. *J. Chem. Phys.* **1993**, *99*, 4597.
(84) van Lenthe, E.; Baerends, E. J.; Snijders, J. G. *J. Chem. Phys.* **1994**, *101*, 9783.
(85) van Lenthe, E.; Snijders, J. G.; Baerends, E. J. *J. Chem. Phys.* **1994**, *105*, 6505.
(86) van Lenthe, E.; van Leeuwen, R.; J., B. E.; Snijders, J. G. *Int. J. Quantum Chem.* **1996**, *57*, 281.
(87) (a) Morokuma, K. *J. Chem. Phys.* **1971**, *55*, 1236. (b) Morokuma, K. *Acc. Chem. Res.* **1977**, *10*, 294. (c) Ziegler, T.; Rauk, A. *Theor. Chim. Acta* **1977**, *46*, 1.
(88) (a) Swart, M.; Solá, M.; Bickelhaupt, F. M. *J. Chem. Phys.* **2009**, *131*, 094103. (b) Swart, M.; Solá, M.; Bickelhaupt, F. M. *J. Comput. Methods Sci. Eng.* **2009**, *9*, 69.
(89) *CrysAlis RED, Program for X-ray CCD camera data reduction* (Version 1.171.32.19); Oxford Diffraction Ltd.: Oxford, United Kingdom, 2008.
(90) Sheldrick, G. M. *SHELXL-97, program for crystal structure determination*; University of Göttingen: Germany, 1997.